Available online at www.sciencedirect.com
ScienceDirect
Journal of Sound and Vibration 308 (2007) 660–673
JOURNAL OF SOUND AND VIBRATION
www.elsevier.com/locate/jsvi

Numerical analysis of fluid–structure interaction effects on vibrations of cantilever microstructure

V. Ostasevicius[a], R. Dauksevicius[a,*], R. Gaidys[b], A. Palevicius[a]

[a]*International Studies Centre, Kaunas University of Technology, A. Mickeviciaus 37, 44244 Kaunas, Lithuania*
[b]*Faculty of Informatics, Kaunas University of Technology, Studentu 50, 51368 Kaunas, Lithuania*

Accepted 27 March 2007
The peer review of this article was organised by the Guest Editor
Available online 29 May 2007

Abstract

The operation of microelectromechanical systems (MEMS) with movable parts is often strongly affected by a fluid–structure interaction. Microelectromechanical devices often operate in ambient pressure, therefore air functions as an important working fluid. The influence of air in MEMS devices manifests as viscous air damping, which can be divided into two categories: slide-film damping and squeeze-film damping. The former occurs in laterally moving devices (e.g. comb drives), while the latter is characteristic for MEMS devices, in which a microstructure moves or bends towards a rigid surface with a thin air film in-between (as in microswitch).

This paper reports results of numerical analysis of squeeze-film damping effects on free and forced vibrations of cantilever microstructure. Three separate finite element models are used for simulations. Each model is based on different form of Reynolds equation: nonlinear, linearized and linearized incompressible. Squeeze-film damping is associated with displacements of microstructure by using weak formulations of the equations that are coupled to lower surface of the microstructure, which is represented in three-dimensional (3D) and is treated as flexible in the analysis. Both small- and large-amplitude motions are considered. Comparison of results obtained with different models is presented and suggestions are given regarding the usage of particular form of Reynolds equation for modelling air-damping effects in the case of developed electrostatic microswitch.

1. Introduction

The performance of microelectromechanical systems (MEMS) with movable parts is often affected by a fluid–structure interaction. Air is the most common fluid in MEMS and usually influence of air in microstructures is associated with dissipative effects. There are several energy dissipation mechanisms that are common in MEMS: (1) losses to surrounding fluid/air due to acoustic radiation, (2) losses due to viscous friction (viscous air damping), (3) losses due to microslips at support (anchor/clamping losses), (4) and intrinsic losses of the material (thermoelastic (internal friction) damping). Among these damping sources, viscous air damping is the most significant source of energy dissipation in MEMS [1]. It may be differentiated

*Corresponding author. Tel.: +370 6826 7170; fax: +370 37323 704.
E-mail address: rolanasd@centras.lt (R. Dauksevicius).

0022-460X/$ - see front matter © 2007 Elsevier Ltd. All rights reserved.
doi:10.1016/j.jsv.2007.03.072

into slide film (or shear) damping, which mainly occurs in laterally moving devices (e.g. comb drives), and squeeze-film damping, which occurs when microstructure moves or bends towards a rigid surface with a thin air film in-between (e.g. in vertical microaccelerometers, micropumps or microswitches). In general, squeeze-film damping is characteristic for MEMS devices that employ parallel-plate capacitors, in which air fills tiny gap between two parallel plates. In order to increase the efficiency of actuation or improve the sensitivity of detection, the distance between the capacitor plates is minimized and the area of the plates is maximized. Consequently, the phenomenon of squeeze-film damping occurs as a result of the massive movement of the air underneath the plate, which is resisted by the viscosity of the air. This gives rise to a pressure distribution underneath the plate, which may act as a spring and/or a damping force. Studies show that the damping force dominates the spring force at low frequencies, whereas the spring force dominates the damping force at high frequencies [2,3].

Reynolds equation known from lubrication technology and theory of rarefied gas physics is the theoretical background to analyse squeezed film effect and damping, which have been studied extensively long before introduction of MEMS [3–6]. Majority of research work on squeeze-film damping in MEMS treats vibrating microstructures as rigid [7–13]. There are only a few models that account for flexibility of microstructures [14–17]. All models are almost exclusively based on linearized Reynolds equation (LRE) [3–7,10–12] or its simplest version—linearized incompressible Reynolds equation (LIRE) [8,9,13]. The models that use nonlinear Reynolds equation (NRE) however frequently approximate a microstructure as one-dimensional (1D) beam [14,16,17]. Only in Ref. [15] NRE is used in conjunction with plate equation.

One of the microdevices in which squeeze-film damping plays a very significant role is a microswitch. A cantilever-type electrostatically actuated microswitch (Fig. 1) was developed at Kaunas University of Technology (KTU) using original nickel surface micromachining technology. Performance of such microswitches combines best attributes that are characteristic to current switching technologies—solid-state devices and conventional electromechanical relays. Since microswitches are contact switches, they have some advantages over PIN diodes and FET switches, namely, lower contact resistance, higher isolation, and better linearity. At the same time, they are much smaller and consume less power than electromechanical relays and are much easier to integrate with electronics. Due to these unique properties, microswitches have the potential to replace electromechanical relays and solid-state devices in significant market areas, particularly in automated test equipment, telecommunication systems, wireless applications and battery-operated equipment [18].

However, microswitches have a few problems that have to be addressed, namely, higher actuation voltage, lower switching speed, reduced lifetime and power handling capabilities [18]. In order to be able to find possible solutions for improvement of these performance parameters a comprehensive mathematical model is required for subsequent analysis and device optimization. The problem of microswitch modelling is truly multidisciplinary and is characterized by high level of complexity since it requires integration of several problems from different disciplines. Development of numerical model of this microdevice is heavily complicated by the fact that its dynamical behaviour is significantly influenced by nonlinear coupling of at least three different energy domains: mechanical, electrical and fluidic. In other words, modelling difficulty

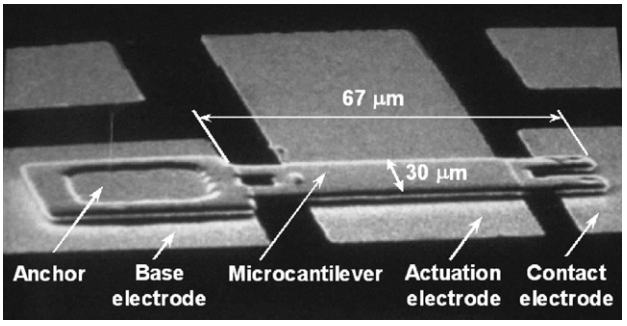

Fig. 1. Picture obtained with scanning electron microscope, which show electrostatically actuated microswitch fabricated at Kaunas University of Technology using original nickel surface-micromachining technology.

is due to the interdependency or interaction of elastic, electrostatic and hydrodynamic effects that determine the dynamics of the microdevice. Fluid–structural interaction in the microswitch manifests in a form of squeeze-film damping, while electrostatic–structural interaction appears as deflection of cantilever microstructure of the microswitch under the influence of applied voltage. Furthermore, since the microswitch is a contact-type device, nonlinear vibro-impact interactions are of great importance and therefore have also to be included into the complete dynamical model. Each of these three interactions found in the microswitch is distinguished by strong nonlinear nature and requires separate analysis.

In this paper, numerical analysis of squeeze-film damping effects on free and forced vibrations of cantilever microstructure is presented. Three separate finite element (FE) models have been developed, each of which is associated with different version of Reynolds equation. The models represent cantilever microstructure in three-dimensional (3D) and the analysis of squeeze-film damping accounts for the flexibility of microstructure. Both small- and large-amplitude motions are considered.

In Chapter 2, summary of main information related to fabricated microswitch is given. Chapter 3 presents three different forms of Reynolds equation, on which constructed FE models are based. In Chapter 4, simulation results obtained with different FE models are compared.

2. Overview of developed microswitch

Microswitch, developed at KTU, is of metal-to-metal type and is actuated electrostatically (Fig. 1). Contacting element of the microswitch is a cantilever microstructure, which is bimetal and is made of upper layer of nickel and lower layer of gold with total thickness of about 2 μm. The width of the microstructure is 30 μm and length ranges from 67 to 150 μm. Spacing between the microstructure and contact electrode (drain) is about 1 μm. Upon application of voltage to actuation electrode (gate), the structure is pulled down by the electrostatic force until the switch closes. When the gate voltage is removed, the restoring force of the structure returns it to its original position.

The microswitch was fabricated using nickel surface micromachining technology. A certain combination of processes such as evaporation, etching, electroplating, etc. was applied in the technological sequence. Special microstructures were formed in the cantilever anchor (support) area by reactive ion etching in order to increase strength of bonding between the cantilever structure and substrate. Different substrates were tested for the fabrication of the device, including semiconductor and dielectric materials. Producing the microswitch on high resistance semiconductor (Si, GaAs, InP) substrate enables its incorporation into semiconductor integrated circuits for switching high power signals, while usage of dielectric (quartz, ceramics) substrate allows to integrate the microswitch into hybrid microelectronic devices.

3. Modelling of squeeze-film damping in a microswitch

One of the major microswitch modelling challenges is associated with fluidic domain. MEMS devices often operate in ambient pressure, therefore air functions as an important working fluid. The influence of fluids in MEMS devices manifests as viscous damping. As gas, such as air, fills the space between MEMS components, viscous air damping strongly affects the dynamic behaviour of these devices. When in operation, cantilever microstructure of the microswitch is undergoing transverse motion with respect to substrate. Since the lateral dimensions of the microstructure are much larger than gap size, its fairly small displacement in normal direction compresses (or pulls back) a significant amount of air out of (or into) the very narrow gap. However, the viscosity of the air film limits the flow rate along the gap, and thus the pressure is increased in the gap and acts against the microstructure. The total pressure force, which opposes the motion of the microstructure, is known as squeeze-film damping [1,2,19].

3.1. Reynolds equation and its versions

On the continuous field level, squeeze-film damping of a microstructure vibrating in a fluid is governed by Navier–Stokes equations, which are solved using computational fluid dynamics methods that are one of the most demanding tasks for FE solvers. Computational time for modelling microswitch dynamic behaviour by

using Navier–Stokes equations and as a part of full system analysis would be excessively long since the full 3D model have to take into account also other highly nonlinear effects such as electrostatic–structural interaction and contact bouncing. Therefore, computational effort required for dynamic simulations using such complicated model would be prohibitive. The most common method to avoid usage of Navier–Stokes equations for modelling squeeze-film damping in MEMS is to apply Reynolds equation, which is used in lubrication theory to determine the behaviour of a thin fluid film between two moving surfaces [20]:

$$\frac{\partial}{\partial x}\left(\frac{\rho h^3}{\mu}\frac{\partial P}{\partial x}\right)+\frac{\partial}{\partial y}\left(\frac{\rho h^3}{\mu}\frac{\partial P}{\partial y}\right)=12\frac{\partial(\rho h)}{\partial t}, \tag{1}$$

where gas density ρ, pressure in the gap p, and the gap thickness h are functions of time and position (x, y). μ is dynamic viscosity of the gas.

Reynolds equation is a nonlinear partial differential equation, which is derived from Navier–Stokes equation, the equation for the conservation of mass and the equation of state for ideal gas by assuming that (1) the fluid is Newtonian (the shear stress is directly proportional to the velocity), (2) the fluid obeys the ideal gas law, (3) the inertia and body forces are negligible compared to the viscous and pressure forces, (4) the variation of pressure across the fluid film is negligibly small, (5) the flow is laminar, (6) the thickness of fluid film is very small compared to the lateral extent of the moving and stationary plates, (7) the fluid can be treated as continuum and does not slip at the boundaries [2,20,21].

Gas is a predominant working fluid in MEMS devices and thin gas films are realistically assumed to be isothermal (i.e. it is assumed that viscous friction does not cause a significant temperature change) since (1) thermal contact between the gas and the surrounding solid surfaces is very good in an MEMS device (volumes are small and surface areas are large), and (2) common MEMS materials are good thermal conductors. The equation of state for an ideal gas gives the density as [20]

$$\frac{P}{\rho}=\bar{R}t_m, \tag{2}$$

where $\bar{R}$ = gas constant = universal gas constant/molecular weight, t_m—gas temperature.

For isothermal process Eq. (2) reduces to [20]

$$\frac{P}{\rho}=\text{constant}. \tag{3}$$

Thus, density in the Reynolds equation can be replaced with pressure. The equation given below is known as isothermal compressible Reynolds equation, however for the sake of brevity it will be further referred to as NRE:

$$\frac{\partial}{\partial x}\left(h^3P\frac{\partial P}{\partial x}\right)+\frac{\partial}{\partial y}\left(h^3P\frac{\partial P}{\partial y}\right)=12\mu\left(h\frac{\partial P}{\partial t}+P\frac{\partial h}{\partial t}\right). \tag{4}$$

The specific condition for the validity of Reynolds equation is [8,22]

$$\frac{\omega h^2\rho}{\mu}\ll 1, \tag{5}$$

where ω is the angular oscillation frequency.

Reynolds equation assumes continuous fluid flow regime. A general measure of acceptance of this assumption is the Knudsen number K_n [18]:

$$K_n=\frac{L_0P_a}{p_0h_0}, \tag{6}$$

where p_0 is the working pressure in the gap, L_0 the mean free path of air particles at ambient pressure P_a and and h_0 the nominal gap height. For the $P_a = 101.325\,\text{kPa}$, $L_0 \approx 65\,\text{nm}$ [21].

Based on the Knudsen number, the flow can be divided into four regimes: continuum flow when $K_n < 0.001$, slip flow when $0.001 < K_n < 0.1$, transitional flow when $0.1 < K_n < 10$, and free molecular flow when $K_n > 10$ [21]. In the continuum regime, the fluid is governed by the Navier–Stokes equations (or equivalently the Reynolds

equation). Many MEMS devices may be designed to operate at very low pressure with a very small gap between the electrodes. Under such conditions, Knudsen number is closer to the noncontinuum regimes. Fortunately, extensive research has extended the validity of Reynolds equation to the noncontinuum regimes, thereby enabling description of the flow using single model. A convenient way to account for gas rarefaction effects is to modify dynamic viscosity μ. Veijola et al. introduced the following fit function of the effective viscosity μ_{eff}, which is valid over a wide range of K_n ($0 \leqslant K_n \leqslant 880$) [7,18]:

$$\mu_{\text{eff}} = \frac{\mu}{1 + 9.638 K_n^{1.159}}. \tag{7}$$

A lot of MEMS devices, such as accelerometers and gyroscopes, are operated in small-amplitude oscillation motions for the sake of signal sensing or optimal performance. Under such circumstances, the Reynolds equation can be linearized into a diffusion-like partial differential equation by assuming that: (1) the displacement of the moving surface is small relative to the film thickness, and (2) pressure variations within the film are small relative to the ambient pressure [2]:

$$\begin{aligned} h &= h_0 + \delta h, \quad \delta h \ll h_0, \\ P &= P_a + \delta P, \quad \delta P \ll P_a, \end{aligned} \tag{8}$$

where P is small pressure variation from the ambient value P_a and h is small variation in gap (gas film) thickness from the initial value h_0.

LRE then may be written in the following form [3,21]:

$$\frac{P_a h_0^2}{12\mu_{\text{eff}}}\left[\frac{\partial^2}{\partial x^2}\left(\frac{\delta P}{P_a}\right) + \frac{\partial^2}{\partial y^2}\left(\frac{\delta P}{P_a}\right)\right] = \frac{\partial}{\partial t}\left(\frac{\delta h}{h_0}\right) + \frac{\partial}{\partial t}\left(\frac{\delta P}{P_a}\right). \tag{9}$$

An important non-dimensional parameter associated with LRE is squeeze number σ [18,21]:

$$\sigma = \frac{12\mu L^2 \omega}{P_a h_0^2}. \tag{10}$$

Squeeze number measures the degree of compression of the air in the gap. At small squeeze numbers ($\sigma \leqslant 3$), i.e. low oscillation frequency of moving structure, viscous damping effect of the air film dominates because the air has enough time to escape the gap without being compressed. At large squeeze numbers (high oscillation frequency), the air film starts to behave like a spring because moving structure is either too big or moving too fast so that the air is trapped in the gap, which gives rise to the compression of the air film. In this case, spring-type behaviour of air film increases structural elasticity of the whole microsystem [2,3,5,6].

It is possible to further simplify LRE by treating the gas in the gap as incompressible. The corresponding LIRE is represented in the following form [8,9,22]:

$$\frac{h_0^3}{12\mu_{\text{eff}}}\left[\frac{\partial^2}{\partial x^2}\left(\frac{\delta P}{P_a}\right) + \frac{\partial^2}{\partial y^2}\left(\frac{\delta P}{P_a}\right)\right] = \frac{\partial h}{\partial t}. \tag{11}$$

In modelling squeeze-film damping effects in the case of microswitch developed at KTU, the original bi-metal complex-shaped cantilevered microstructure at this stage of numerical analysis is approximated as ideal homogeneous cantilever microstructure with material properties of bulk nickel that is suspended a few microns over the ground thus making an air gap in-between. Structural damping is assumed to be zero in the analysis. Commercially-available FE solver Comsol Multiphysics is used for modelling and simulation. The parameters selected for numerical simulations are as follows: cantilever length $L = 117\,\mu\text{m}$, width $w = 30\,\mu\text{m}$, thickness $t = 2\,\mu\text{m}$, modulus of elasticity $E = 207 \times 10^9\,\text{N/m}^2$, Poisson's ratio $v = 0.31$, density $\rho = 8902\,\text{kg/m}^3$. Due to symmetry only half of the microstructure is modelled (Fig. 2). In order to link squeeze-film damping with the displacements of the microstructure weak formulations of three different variations of Reynolds equation are used, that are "coupled" to lower surface of the cantilever. Thus, in total, three separate FE models have been developed each having the same microstructure associated with different version of Reynolds equation: NRE, LRE and LIRE. The following parameters are used in association with

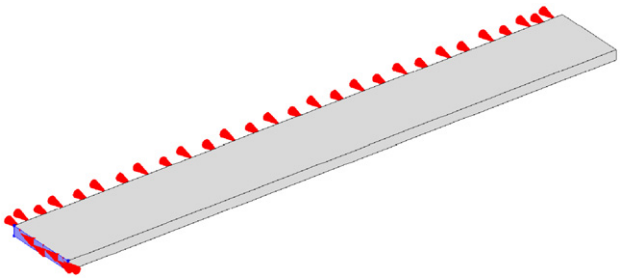

Fig. 2. Finite element half-symmetry model of cantilever microstructure. Special symbols located next to the structure indicate boundary conditions (clamping of one end and constraint of symmetry plane).

Reynolds equations: dynamic viscosity of air $\mu = 18.3 \times 10^{-6}$ Pa s, ambient pressure $P_a = 101.325$ kPa, mean free path of air particles at atmospheric pressure $L_0 = 65$ nm.

4. Numerical simulation results

4.1. Free vibrations of cantilever microstructure

In order to make cantilever microstructure vibrate freely, its bottom-end edge was displaced upwards a certain distance and then released. A series of transient analyses were performed, which purpose was to determine influence of air on free vibrations of the microstructure after it has been released from its initial deflected position. From Figs. 3 and 4, it is obvious that level of working pressure in the gap p_0 as well as gap thickness h_0 have a significant effect on level of damping of the microstructure: effect of squeeze-film damping intensifies with increase in working pressure and decrease in gap thickness. As an example, Fig. 5 shows pressure distribution in the gap with air at atmospheric pressure after 30 μs of simulation. The convex profile of pressure distribution indicates areas of increased pressure in the gap above the atmospheric. In these areas, squeeze-film phenomenon is mostly pronounced and the pressure cycle changes from compression to decompression while the microstructure is undergoing periodic motion. Observing the figure reveals that near the edges of the microstructure pressure is equal to atmospheric. Simulation results presented in Figs. 3 and 4 were obtained by using model with LIRE and large-displacement free vibrations (ratio between gap thickness and initial deflection magnitude $h_0/z = 1$). Calculations analogous to those in Fig. 3 were also performed with NRE. Comparing the x-coordinate of amplitude peaks of curves corresponding to different levels of working pressure in Figs. 3 and 6 it can be noticed that in the case of model with NRE, the x-coordinate of the peak increases with decrease in pressure. In the case of model with LIRE, the peak position on x-axis is constant. The x-coordinate of amplitude peaks also changes when model with NRE undergoes small-amplitude free vibrations ($h_0/z = 100$) (Fig. 7), however the variation is not so obvious. This particular behaviour of variation of x-coordinate of amplitude peaks could be attributed to nonlinearities that are induced in the case of model with NRE and which are more pronounced in the case of large-amplitude free vibrations.

Multiple simulations were carried out with different squeeze-film damping models in order to compare the level of damping that each model generates under different working pressure in the gap in the case of free vibrations. Damping ratios were subsequently extracted from the obtained decaying vibration curves by using the following equation [23]:

$$\zeta = \frac{\Delta}{\sqrt{4\pi^2 + \Delta^2}}, \tag{12}$$

where ζ is the damping ratio and Δ the logarithmic decrement.

Results of this analysis are summarized in Fig. 8, which reveals that for the case of free vibrations, amount of induced squeeze-film damping estimated with different models is very similar, only difference between NRE, LRE and LIRE being more pronounced. It is obvious from the graph that LIRE underestimates damping in comparison to LRE and NRE. Though hardly discernible in Fig. 8, but the calculations indicate

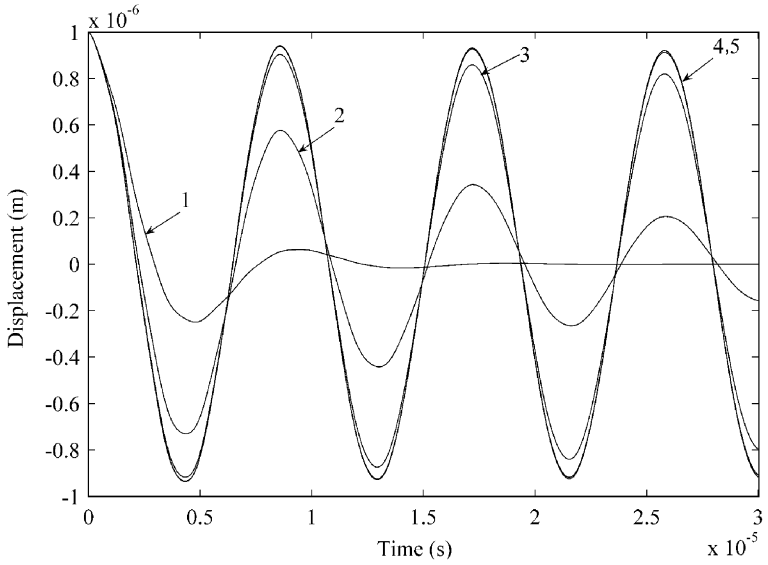

Fig. 3. Simulated results from model with LIRE showing free vibration response curves of the arbitrary point at the end of a cantilever microstructure after it has been released from its initial deflected position $z = 1\,\mu m$ upwards for the different levels of working air pressure p_0 in the gap with thickness $h = 1\,\mu m$. Curves: 1 – 10^5 Pa, 2 – 10^4 Pa, 3 – 10^3 Pa, 4 – 10^2 Pa, 5 – 10 Pa.

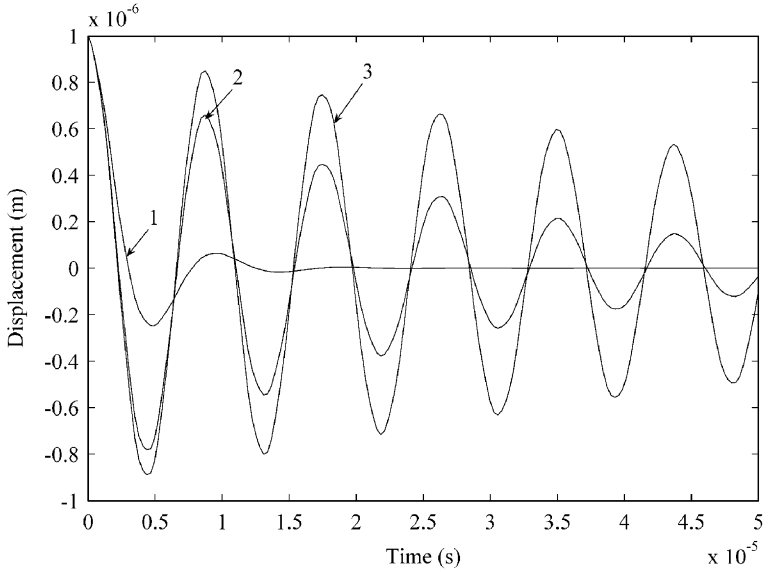

Fig. 4. Simulated results from model with LIRE showing free vibration response curves of the arbitrary point at the end of the cantilever microstructure after it has been released from its initial deflected position $z = 1\,\mu m$ upwards at the fixed working pressure of $p_0 = 10^5$ Pa but for different values of gap thickness h_0. Curves: 1 – 1 μm, 2 – 2 μm, 3 – 3 μm.

that the largest difference in damping ratios between NRE and LIRE is obtained for working pressures $p_0 = 100$ and 1000 Pa (13% and 17%, respectively). The average difference between damping ratios in the case of NRE and LRE is just 0.7%.

4.2. Forced vibrations of cantilever microstructure

For the evaluation of squeeze-film damping effects in the case of forced vibrations, bottom-end edge of cantilever microstructure was excited with sinusoidal force $F_a \sin(2\pi ft)$. During the numerical analysis effects

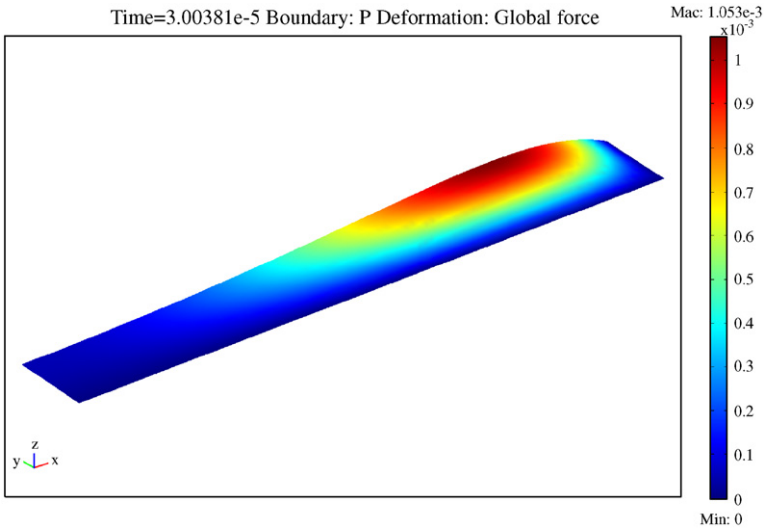

Fig. 5. Pressure distribution in the gap with air at atmospheric pressure after 30 μs of simulation of free vibrations of cantilever microstructure.

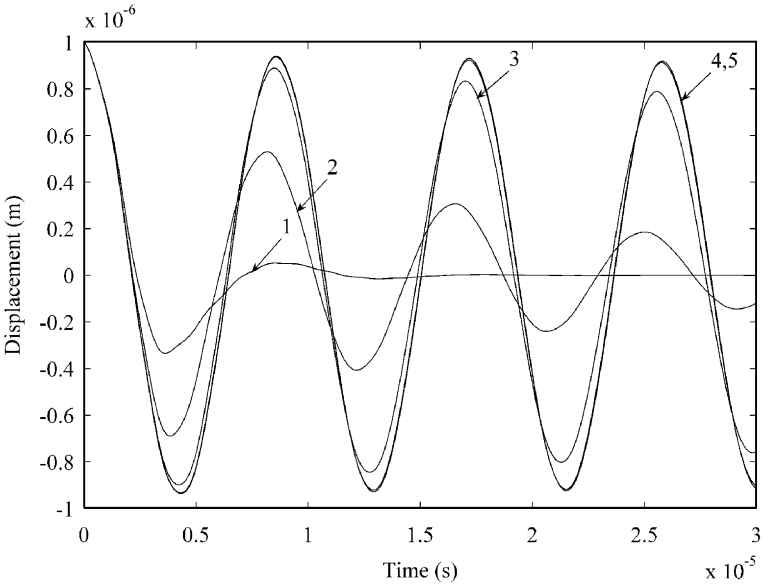

Fig. 6. Simulated results from model with NRE showing free vibration response curves of the arbitrary point at the end of a cantilever microstructure after it has been released from its initial deflected position $z = 1\,\mu m$ upwards for the different levels of working air pressure p_0 in the gap with thickness $h = 1\,\mu m$. Curves: 1 – 10^5 Pa, 2 – 10^4 Pa, 3 – 10^3 Pa, 4 – 10^2 Pa, 5 – 10 Pa.

of small- and large-amplitude motions (achieved by selecting appropriate force amplitude F_a) as well as influence of different excitation frequency f on squeeze-film damping were predicted. During the simulations working pressure in the gap was constant and set to $p_0 = 10^5$ Pa.

Time response of arbitrary end point of cantilever microstructure was investigated with all three damping models in the case when the microstructure was excited with force, which frequency is equal to fundamental frequency of microstructure ($f_1 = 116.3$ kHz). When sinusoidal excitation of this frequency is applied to microstructure without Reynolds equation coupled to it (i.e. without damping), then we obtain amplitude

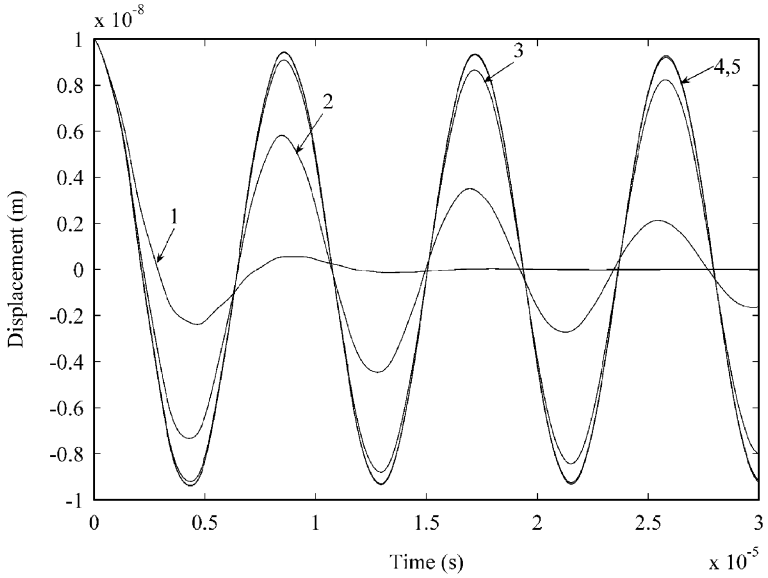

Fig. 7. Simulated results from model with NRE showing free vibration response curves of the arbitrary point at the end of a cantilever microstructure after it has been released from its initial deflected position $z = 0.01\,\mu m$ upwards for the different levels of working air pressure p_0 in the gap with thickness $h = 1\,\mu m$. Curves: 1 – 10^5 Pa, 2 – 10^4 Pa, 3 – 10^3 Pa, 4 – 10^2 Pa, 5 – 10 Pa.

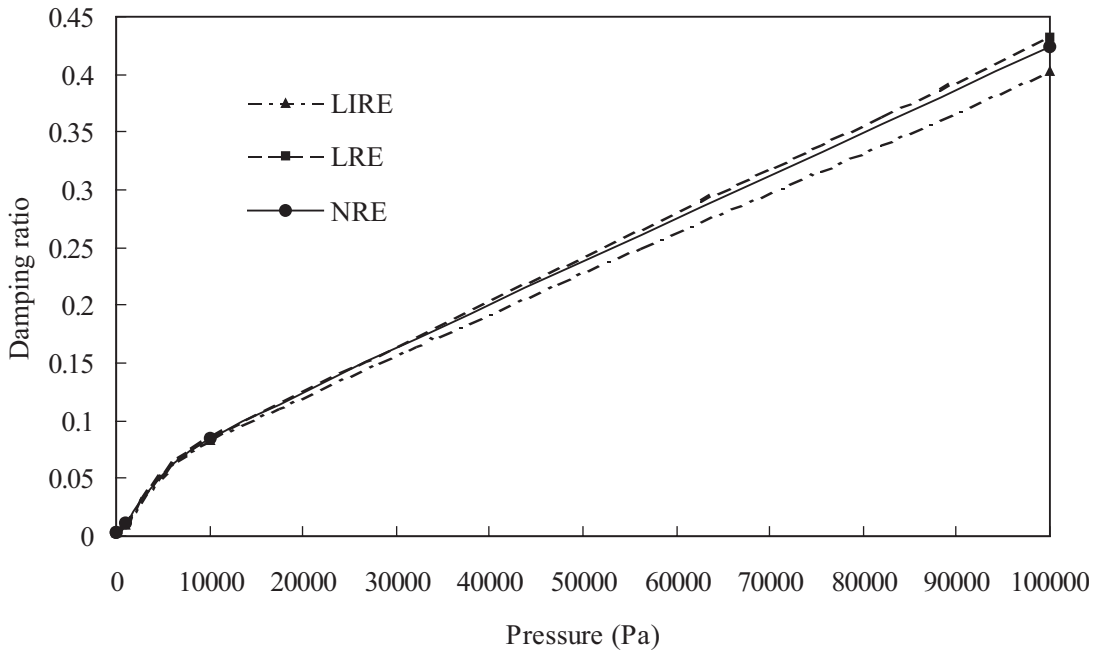

Fig. 8. Comparison of variation of damping ratios obtained by using different squeeze-film damping models and by extracting them from simulated free vibration response curves of the arbitrary point at the end of a cantilever microstructure after it has been released from its initial deflected position $z = 1\,\mu m$ upwards for the different levels of working air pressure p_0 in the gap with thickness $h = 1\,\mu m$.

increase without bound producing resonance (Fig. 9). Fig. 10 shows time response of arbitrary end point of cantilever microstructure when it is excited with sinusoidal force of the magnitude that produces small-amplitude vibrations ($h_0/z \approx 70$) and which frequency equals to fundamental one in the presence of squeeze-film damping modelled with LIRE, LRE and NRE. It is obvious that curves obtained with different models

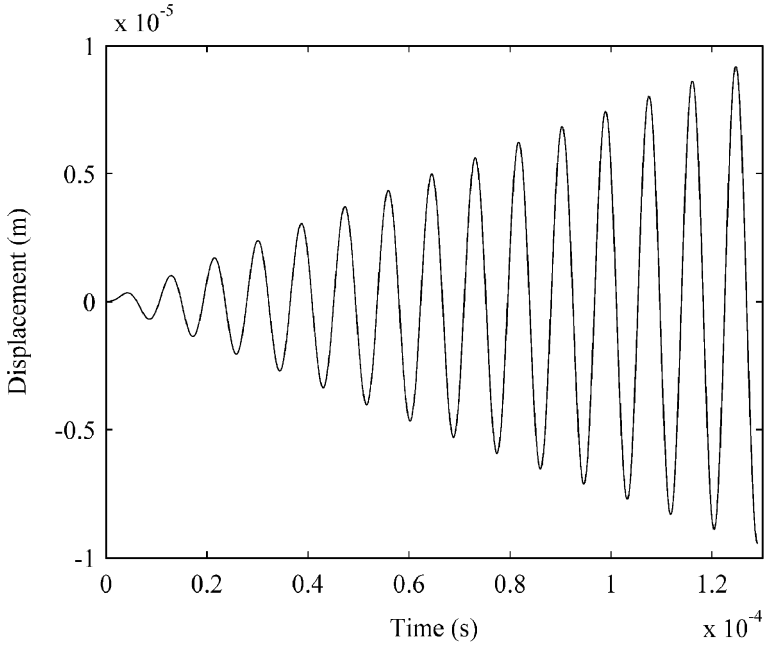

Fig. 9. Simulated response of arbitrary end point of undamped microstructure (without squeeze-film damping) excited with sinusoidal force, which frequency equals to fundamental frequency of microstructure.

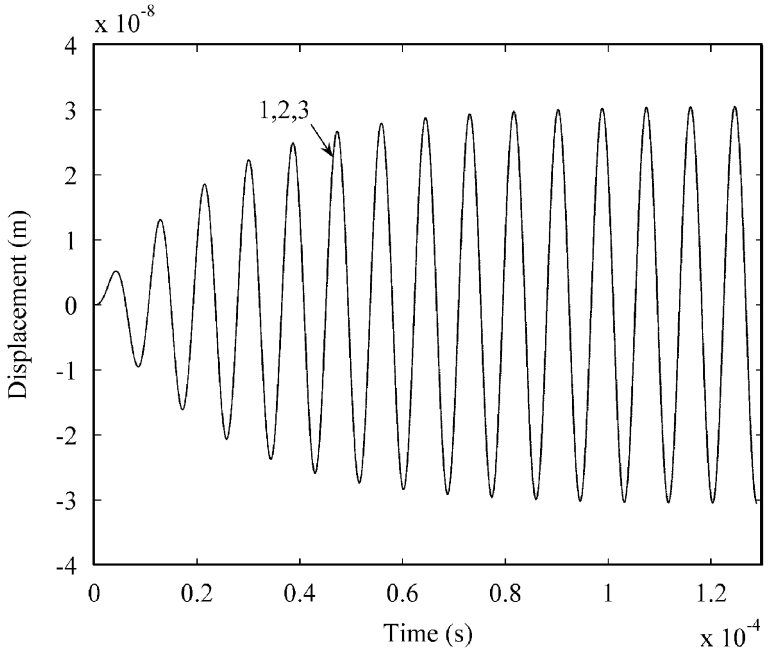

Fig. 10. Time response of arbitrary end point of cantilever microstructure excited with sinusoidal force of the magnitude that produces small-amplitude vibrations ($h_0/z \approx 70$) and which frequency equals to fundamental frequency of microstructure in the presence of squeeze-film damping modelled with LIRE (1), LRE (2) and NRE (3). Gap thickness $h_0 = 2\,\mu m$, working pressure in the gap $p_0 = 10^5\,Pa$.

coincide very closely. However, different results are observed when magnitude of sinusoidal excitation force is increased so as to generate large-displacement vibrations (Fig. 11). From the curves one may determine that response amplitude for the model with LIRE is about 35% larger than with LRE and NRE. This leads to the

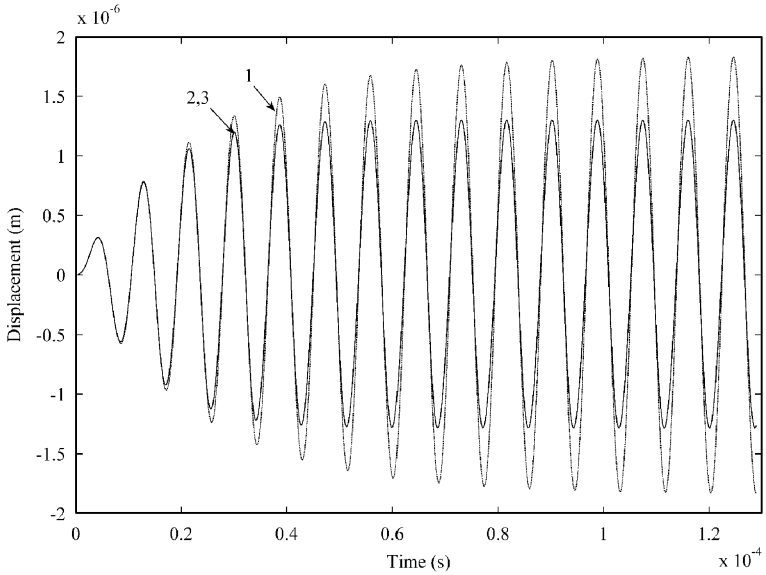

Fig. 11. Time response of arbitrary end point of cantilever microstructure excited with sinusoidal force of the magnitude that produces large-amplitude vibrations and which frequency equals to fundamental frequency of microstructure in the presence of squeeze-film damping modelled with LIRE (1), LRE (2) and NRE (3). Gap thickness $h_0 = 2\,\mu m$, working pressure in the gap $p_0 = 10^5\,Pa$.

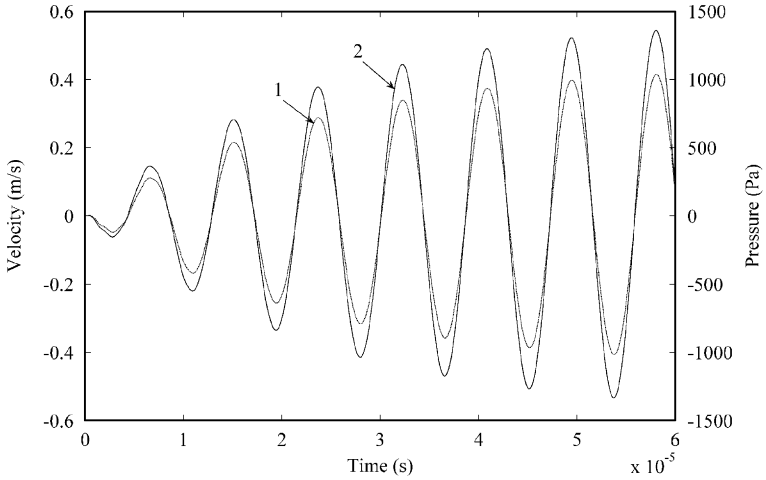

Fig. 12. Comparison of time responses of velocity (1) and pressure (2) at arbitrary midpoint of cantilever microstructure excited with sinusoidal force of the magnitude that produces large-amplitude vibrations and which frequency equals to fundamental frequency of microstructure in the presence of squeeze-film damping modelled with LIRE. Gap thickness $h_0 = 2\,\mu m$, working pressure in the gap $p_0 = 10^5\,Pa$.

conclusion that model with LIRE significantly underestimates squeeze-film damping of microstructure in comparison to models with LRE and NRE, which results again match very well.

A series of simulations were performed in order to compare transient responses of velocity and pressure at arbitrary midpoint of cantilever microstructure excited with sinusoidal force of the magnitude that produces large-amplitude vibrations in the presence of squeeze-film damping modelled with LIRE (Fig. 12) and NRE (Fig. 13). The figures reveal obvious differences in the models. Fig. 13 indicates a nonlinear pressure response for large-amplitude motion.

It is well known that in the case of squeeze-film phenomenon pressure force exerted by the air film undergoing periodic cycles of compression and decompression has two components: one is in phase with

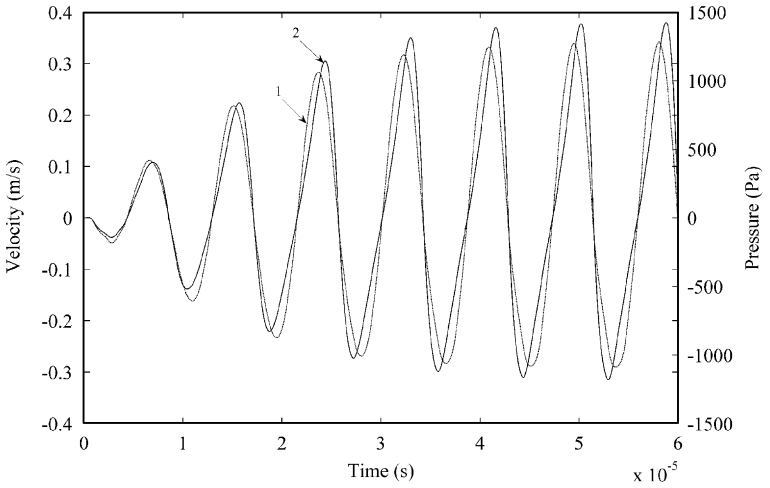

Fig. 13. Comparison of responses of velocity (1) and pressure (2) at arbitrary midpoint of cantilever microstructure excited with sinusoidal force of the magnitude that produces large-amplitude vibrations and which frequency equals to fundamental frequency of microstructure in the presence of squeeze-film damping modelled with NRE. Gap thickness $h_0 = 2\,\mu m$, working pressure in the gap $p_0 = 10^5\,Pa$.

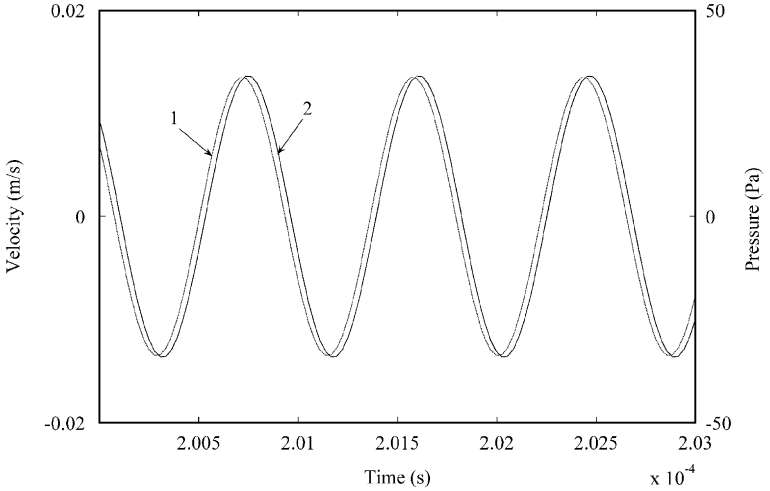

Fig. 14. Comparison of responses of velocity (1) and pressure (2) at arbitrary midpoint of cantilever microstructure excited with sinusoidal force of the magnitude that produces small-amplitude vibrations and which frequency equals to $10f_1$ in the presence of squeeze-film damping modelled with NRE. Gap thickness $h_0 = 2\,\mu m$, working pressure in the gap $p_0 = 10^5\,Pa$.

velocity (i.e. viscous damping force) and the other is in phase with plate displacement (i.e. the spring force due to compressibility of air). At relatively low oscillation frequencies or relatively large air gaps (small squeeze number σ), the viscous damping force dominates because the air can squeeze out of the gap without being compressed. While, at relatively high frequencies or relatively small gaps (large squeeze number σ), spring forces increase because of the compression of the air film. In such conditions, the film becomes virtually non-dissipative, showing a nonlinear spring action. In practice, the air film represents a combination of viscous damping and spring forces [2,3,5,6,14].

Therefore, simulations were performed during which frequency of sinusoidal excitation force was varied in the course of numerical analysis in order to study its influence on character of squeeze-film damping and emphasize differences between the models. Figs. 14 and 15 present transient responses of velocity (1) and pressure (2) at arbitrary midpoint of cantilever microstructure excited with sinusoidal force of the magnitude that produces small-amplitude vibrations and which frequency is 10 (Fig. 14) and 100 (Fig. 15) times larger

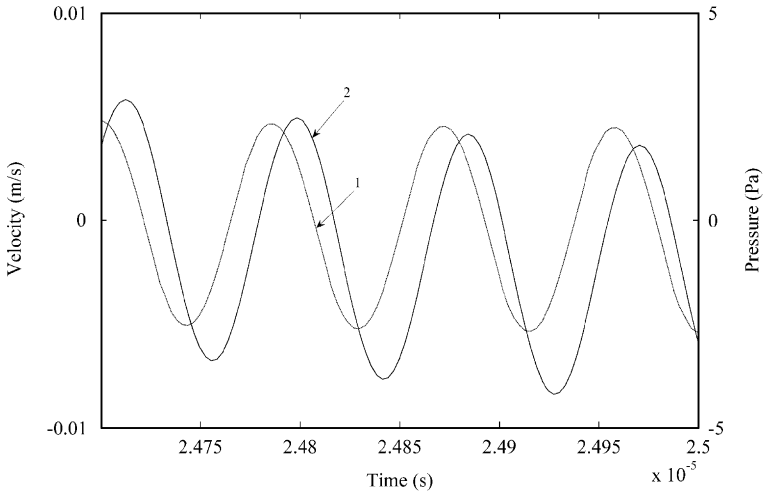

Fig. 15. Comparison of responses of velocity (1) and pressure (2) at arbitrary midpoint of cantilever microstructure excited with sinusoidal force of the magnitude that produces small-amplitude vibrations and which frequency equals to $100f_1$ in the presence of squeeze-film damping modelled with NRE. Gap thickness $h_0 = 2\,\mu m$, working pressure in the gap $p_0 = 10^5\,Pa$.

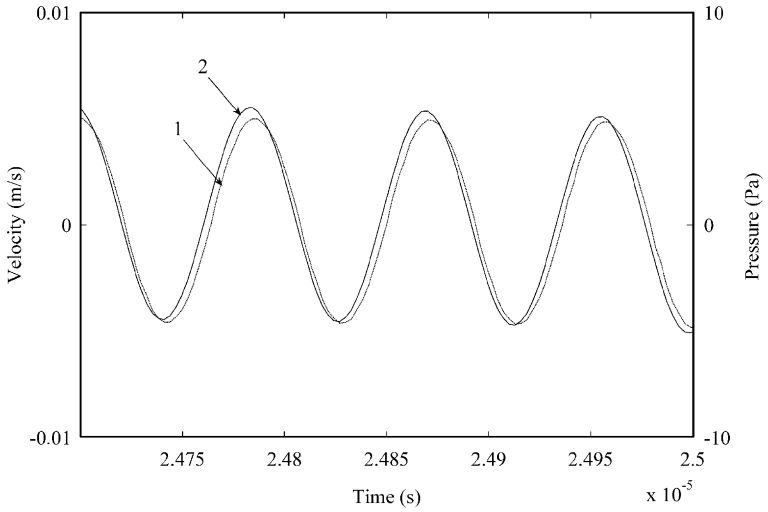

Fig. 16. Comparison of responses of velocity (1) and pressure (2) at arbitrary midpoint of cantilever microstructure excited with sinusoidal force of the magnitude that produces small-amplitude vibrations and which frequency equals to $100f_1$ in the presence of squeeze-film damping modelled with LIRE. Gap thickness $h_0 = 2\,\mu m$, working pressure in the gap $p_0 = 10^5\,Pa$.

than fundamental frequency of microstructure in the presence of squeeze-film damping modelled with NRE. From the figures one may clearly notice that the pressure lags behind the sinusoidal velocity and that the phase lag increases with vibration frequency, which in turn indicates decrease in viscous damping forces and increase in spring forces. In contrast, such tendency is not observed for the analogous simulation (excitation frequency is $f = 100f_1$) but using model with LIRE (Fig. 16). This result is natural since LIRE neglects air compressibility effects. Here, pressure and velocity are approximately in phase, even we may notice that pressure somewhat leads the velocity.

5. Conclusions

The results of study of squeeze-film damping effects on free and forced vibrations of cantilever microstructure are reported in the paper. Simulations were performed with three separate FE models, each

using the same 3D flexible microstructure but coupled with Reynolds equation of different approximation level, represented in the weak form within the commercial FEM package.

Numerical analysis of influence of air damping on free vibrations of microstructure indicate increase in damping factor with increase of pressure in the gap and decrease or air film thickness. Comparison of damping factors estimated from simulations carried out with different squeeze-film damping models show minor differences between results from NRE- and LRE-based models. Simulations of free vibrations and large-amplitude forced vibrations revealed that incompressible form of LRE underestimates level of air damping in comparison to other two equations. Nonlinear character of pressure response with respect to velocity response of arbitrary midpoint of microstructure is observed in the case of simulations with NRE-based model. Study of influence of sinusoidal excitation frequency on small-amplitude forced vibrations of microstructure indicates that air compressibility effects become more pronounced with increase in excitation frequency. This is not observed in the case of FE model coupled with LIRE.

It is obvious from performed numerical analysis that LIRE oversimplifies the phenomenon of squeeze-film damping, particularly in the case of large-amplitude vibrations of microstructure. Therefore, the use of NRE or LRE is suggested for modelling air damping effects in the microswitch. Further research is necessary in order to highlight differences between these two forms of Reynolds equation.

References

[1] R.M. Lin, W.J. Wang, Structural dynamics of microsystems—current state of research and future directions, *Mechanical Systems and Signal Processing* 20 (2006) 1015–1043.

[2] S.D. Senturia, *Microsystem Design*, Kluwer Academic Publishers, Dordrecht, 2001.

[3] J.J. Blech, On isothermal squeeze films, *Journal of Lubrication Technology* 105 (1983) 615–620.

[4] W.E. Langlois, Isothermal squeeze films, *Quarterly Applied Mathematics* XX (2) (1962) 131–150.

[5] W.S. Griffin, H.H. Richardson, S. Yamanami, A study of fluid squeeze-film damping, *Journal of Basic Engineering—Transactions of the ASME* (1966) 451–456.

[6] M.H. Shadd, A.K. Stiffler, Squeeze film dampers: amplitude effects at low squeeze numbers, *Journal of Engineering for Industry—Transactions of the ASME* (1975) 1366–1370.

[7] T. Veijola, H. Kuisma, J. Lahdenpera, T. Ryhanen, Equivalent circuit model of the squeezed gas film in a silicon accelerometer, *Sensors and Actuators A* 48 (1995) 239–248.

[8] J.B. Starr, Squeeze-film damping in solid-state accelerometers, *Proceeding of the IEEE Solid-State Sensor and Actuator Workshop*, Hilton Head Island, South Carolina, 1990, pp. 44–47.

[9] M. Bao, H. Yang, Y. Sun, P.J. French, Modified Reynolds' equation and analytical analysis of squeeze-film air damping of perforated structures, *Journal of Microemechanics and Microengineering* 13 (2003) 795–800.

[10] M. Andrews, I. Harris, G. Turner, A comparison of squeeze-film theory with measurements on a microstructure, *Sensors and Actuators A* 36 (1) (1993) 79–87.

[11] R.B. Darling, C. Hivick, J. Xu, Compact analytical modeling of squeeze film damping with arbitrary venting conditions using a Green's function approach, *Sensors and Actuators A* 70 (1–2) (1998) 32–41.

[12] W.-M. Zhang, G. Meng, H.-G. Li, Modeling and simulation of the squeeze film effect on the MEMS structures, *Microwave Conference Proceedings, APMC 200, Asia-Pacific Conference Proceedings*, Vol. 2, 2005, 3pp.

[13] P.B. Chu, P.R. Nelson, M.L. Tachiki, K.S. Pister, Dynamics of polysilicon parallel-plate electrostatic actuators, *Sensors and Actuators A* 52 (1996) 216–220.

[14] Y.J. Yang, S.D. Senturia, Numerical simulation of compressible squeezed-film damping, *Technical Digest of Solid State Sensor and Actuator Workshop*, Hilton Head Island, South Carolina, 1996, pp. 76–79.

[15] A.H. Nayfeh, M.I. Younis, A new approach to the modeling and simulation of flexible microstructures under the effect of squeeze-film damping, *Journal of Microemechanics and Microengineering* 14 (2004) 170–181.

[16] B. McCarthy, G. Adams, N. McGruer, D. Potter, A dynamic model, including contact bounce of an electrostatically actuated microswitch, *Journal of Microelectromechanical Systems* 11 (2002) 276–283.

[17] E.S. Hung, S.D. Senturia, Generating efficient dynamical models for microelectromechanical systems from a few finite-element simulations runs, *Journal of Microelectromechanical Systems* 8 (1999) 280–289.

[18] G.B. Rebeiz, *RF MEMS: Theory, Design, and Technology*, Wiley-Interscience, New York, 2003.

[19] J.A. Pelesko, D.H. Bernstein, *Modeling MEMS and NEMS*, Chapman & Hall, London, 2003 CRC, Boca Raton, FL.

[20] B.J. Hamrock, S.R. Schmid, B.O. Jacobson, *Fundamentals of Fluid Film Lubrication*, McGraw-Hill, New York, 2004.

[21] M. Gad-el-Hak, *MEMS Handbook*, CRC Press, Boca Raton, FL, 2002.

[22] FEMLAB 3.2 MEMS Module Model Library, 2005.

[23] S.G. Kelly, *Fundamentals of Mechanical Vibrations*, McGraw-Hill, New York, 2000.